

Analysis of rare driving events in pediatric acute myeloid leukemia

Sanne Noort,¹ Jolieke van Oosterwijk,² Jing Ma,³ Elizabeth A.R. Garfinkle,⁴ Stephanie Nance,⁴ Michael Walsh,³ Guangchun Song,³ Dirk Reinhardt,⁵ Martina Pigazzi,⁶ Franco Locatelli,⁷ Henrik Hasle,⁸ Jonas Abrahamsson,⁹ Marie Jarosova,¹⁰ Charikleia Kelaidi,¹¹ Sophia Polychronopoulou,¹¹ Marry M. van den Heuvel-Eibrink,¹² Maarten Fornerod,¹³ Tanja A. Gruber⁴ and C. Michel Zwaan^{1,12}

¹Pediatric Oncology/Hematology, Erasmus MC-Sophia Children's Hospital, Rotterdam, the Netherlands; ²US Biologic, Inc, Memphis, TN, USA; ³Department of Pathology, St. Jude Children's Research Hospital, Memphis, TN, USA; ⁴Department of Oncology, St. Jude Children's Research Hospital, Memphis, TN, USA; ⁵AML-BFM Study Group, Pediatric Hematology and Oncology, Essen, Germany; ⁶Women and Child Health Department, Hematology-Oncology Clinic and Lab, University of Padova, Padova, Italy; ⁷Italian Association of Pediatric Hematology and Oncology, University of Pavia, Pavia, Italy; ⁸Pediatrics and Adolescent Medicine, Aarhus University Hospital, Aarhus, Denmark; ⁹Nordic Society for Pediatric Hematology and Oncology, Department of Pediatrics, Institution for Clinical Sciences, Sahlgrenska Academy, University of Gothenburg, Gothenburg, Sweden; ¹⁰Center of Molecular Biology and Gene Therapy, Department of Internal Hematology and Oncology, Masaryk University Hospital, Brno, Czech Republic; ¹¹Department of Pediatric Hematology and Oncology, "Aghia Sophia" Children's Hospital, Athens, Greece; ¹²Princess Máxima Center for Pediatric Oncology, Utrecht, the Netherlands and ¹³Department of Cell Biology, Erasmus MC, Rotterdam, the Netherlands

Correspondence: C. M. Zwaan
c.m.zwaan@erasmusmc.nl


Received: November 29, 2021.

Accepted: July 19, 2022.

Prepublished: July 28, 2022.

<https://doi.org/10.3324/haematol.2021.280250>

©2023 Ferrata Storti Foundation

Published under a CC BY-NC license 

Abstract

Elucidating genetic aberrations in pediatric acute myeloid leukemia (AML) provides insight in biology and may impact on risk-group stratification and clinical outcome. This study aimed to detect such aberrations in a selected series of samples without known (cyto)genetic aberration using molecular profiling. A cohort of 161 patients was selected from various study groups: DCOG, BFM, SJCRH, NOPHO and AEIOP. Samples were analyzed using RNA sequencing (n=152), whole exome (n=135) and/or whole genome sequencing (n=100). In 70 of 156 patients (45%), of whom RNA sequencing or whole genome sequencing was available, rearrangements were detected, 22 of which were novel; five involving *ERG* rearrangements and four *NPM1* rearrangements. *ERG* rearrangements showed self-renewal capacity *in vitro*, and a distinct gene expression pattern. Gene set enrichment analysis of this cluster showed upregulation of gene sets derived from Ewing sarcoma, which was confirmed comparing gene expression profiles of AML and Ewing sarcoma. Furthermore, *NPM1*-rearranged cases showed cytoplasmic NPM1 localization and revealed *HOXA/B* gene overexpression, as described for *NPM1* mutated cases. Single-gene mutations as identified in adult AML were rare. Patients had a median of 24 coding mutations (range, 7-159). Novel recurrent mutations were detected in *UBTF* (n=10), a regulator of RNA transcription. In 75% of patients an aberration with a prognostic impact could be detected. Therefore, we suggest these techniques need to become standard of care in diagnostics.

Introduction

Acute myeloid leukemia (AML) is a rare disease in children. Over the last decades survival has reached a plateau with current event-free survival (EFS) rates of approximately 50-65% and overall survival (OS) over 70% using contemporary protocols.¹⁻³ Currently, pediatric AML patients are treated with four or five courses of chemotherapy followed by hematopoietic stem cell transplantation in high risk cases.² Treatment stratification is mainly based on early

treatment response and genetic abnormalities.⁴ Further chemotherapy intensification is not feasible as treatment toxicity results in a 5-10% mortality rate.⁵ Therefore, improved treatment stratification or novel, preferably targeted, therapeutic options are necessary.

Pediatric AML is a heterogeneous disease characterized by various type I and type II aberrations.⁶ Type I aberrations generally result in a proliferation advantage, such as mutations in *N/KRAS*, and *FLT3*-ITD, which are not mutually exclusive.^{7,8} Type II aberrations generally result in a differ-

entiation block, occur early in leukemic development and are mutually exclusive, such as *KMT2A*-rearrangements, *RUNX1-RUNX1T1* and *CBFB-MYH11*.⁹ Type II aberrations have been reported to be important predictors of outcome.⁷ In recent years, research focused on refining the risk group stratification and elucidating genetic aberrations in what was previously conceived as '(cyto-)genetically normal' AML.^{7,10-12} For instance, Hollink et al. described cytogenetically cryptic *NUP98-NSD1* rearrangements as a novel recurrent unfavorable prognostic rearrangement in pediatric AML.¹² Furthermore, De Rooij et al. used next-generation sequencing (NGS) to characterize non-DS acute megakaryoblastic leukemia (AMKL), a subtype of AML which is associated with a poor outcome,¹¹ and identified *HOX* gene rearrangements with a favorable outcome. Translocations were found in approximately 82% of pediatric AMKL patients.¹¹ In adult AML, genomic profiling revealed recurrent single gene mutations such as *NPM1*, *CEBPA*, *RUNX1* and *DNMT3A*, which have distinct prognostic significance.¹³ These single gene mutations are rare in children, further underlining that pediatric AML could be a primarily fusion-driven disease.¹⁴⁻¹⁶ Despite these advances, approximately 25% of pediatric AML patients still present with unknown somatic genetic abnormalities.

In the current study, we aimed to identify novel driving oncogenic events in pediatric AML patients without a known type II aberration by karyotype and/or other molecular analysis. NGS, RNA sequencing (RNAseq), whole exome sequencing (WES) and whole genome sequencing (WGS), was performed on primary pediatric AML samples.

Methods

Patient selection

Patients (n=161) were selected from five different study groups: St Jude Children's Research Hospital (SJCRH), the Dutch Childhood Oncology Group (DCOG), the Berlin-Frankfurt-Münster group (BFM), the Nordic Society of Pediatric Hematology and Oncology (NOPHO), and the Associazione Italia di Ematologica e Oncologia Pediatrica (AIEOP) (Figure 1; *Online Supplementary Table S1*). Each research group selected patients for this study according to their own diagnostic standard work-up (*Online Supplementary Appendix*). This study was approved by the ethics committee of each research group.

Next-generation sequencing

RNAseq, WGS and WES were performed as previously described.¹¹ Data has been published previously by Fornerod et al.¹⁷ Fusions detected by RNAseq or WGS were validated by reverse transcription polymerase chain reaction (RT-PCR). Single nucleotide variant (SNV) calls were considered valid if they were detected by at least two NGS tech-

niques. Only Insertions and deletions in a genome (indels) with at least five reads in the AML sample and no reads in the germline sample were considered as valid mutations, in samples where only WES or WGS was performed. If only one NGS technique was available, also SNV calls with at least five reads in the AML sample and no reads in the germline sample were considered as valid mutations.

Gene expression analysis

Gene expression analysis was performed as described previously.¹¹ Briefly, fragments per kilobase of transcript per million mapped reads (FPKM) were used. Genes that were not expressed in any sample group were excluded from the final data matrix for downstream analysis, i.e., FPKM value ≥ 0.5 . Only mRNA was used in the analysis and mRNA encoded by sex-specific genes were excluded.¹¹ Downstream analysis was performed using R, version 3.6.1. Differential gene expression was performed using Voom (*Online Supplementary Appendix*).¹⁸ For gene set enrichment analysis (GSEA), genes were ranked based on t-statistic and analyzed using the Broad Institute GSEA Desktop Application version 2.2.4.^{19,20}

NPM1 immunofluorescence

NPM1 immunofluorescence was performed on cytopins of pediatric AML samples and one healthy control, using the anti-NPM1 antibody FC-61911 (Invitrogen, Paisley, UK) and DAPI to stain the nuclei (*Online Supplementary Appendix*).

Serial colony-replating assay

For functional validation of novel aberrations, serial colony replating was performed. Lineage depleted bone marrow cells derived from 6-8 week old BL6 mice were prepared and transduced as previously described¹¹ (*Online Supplementary Appendix*).

Statistical analysis

Analysis were performed using R, version 3.6.1. All tests were 2-tailed, and a *P* value < 0.05 was considered significant. Complete remission (CR) was defined as $< 5\%$ blasts in the bone marrow, with regeneration of trilineage hematopoiesis and no leukemic cells in cerebrospinal fluid or elsewhere. If a patient did not reach CR, treatment was considered a failure at day 0. Overall survival (OS) was calculated from the day of diagnosis until the date of last follow-up or death from any cause. Event-free survival (EFS) was measured from the day of diagnosis to the date of the first event or the date of last follow-up. Events considered in this analysis were resistant disease, relapse, occurrence of secondary malignancy and death. Kaplan-Meier curves for OS and EFS were calculated and plotted using the survival package in R.²¹

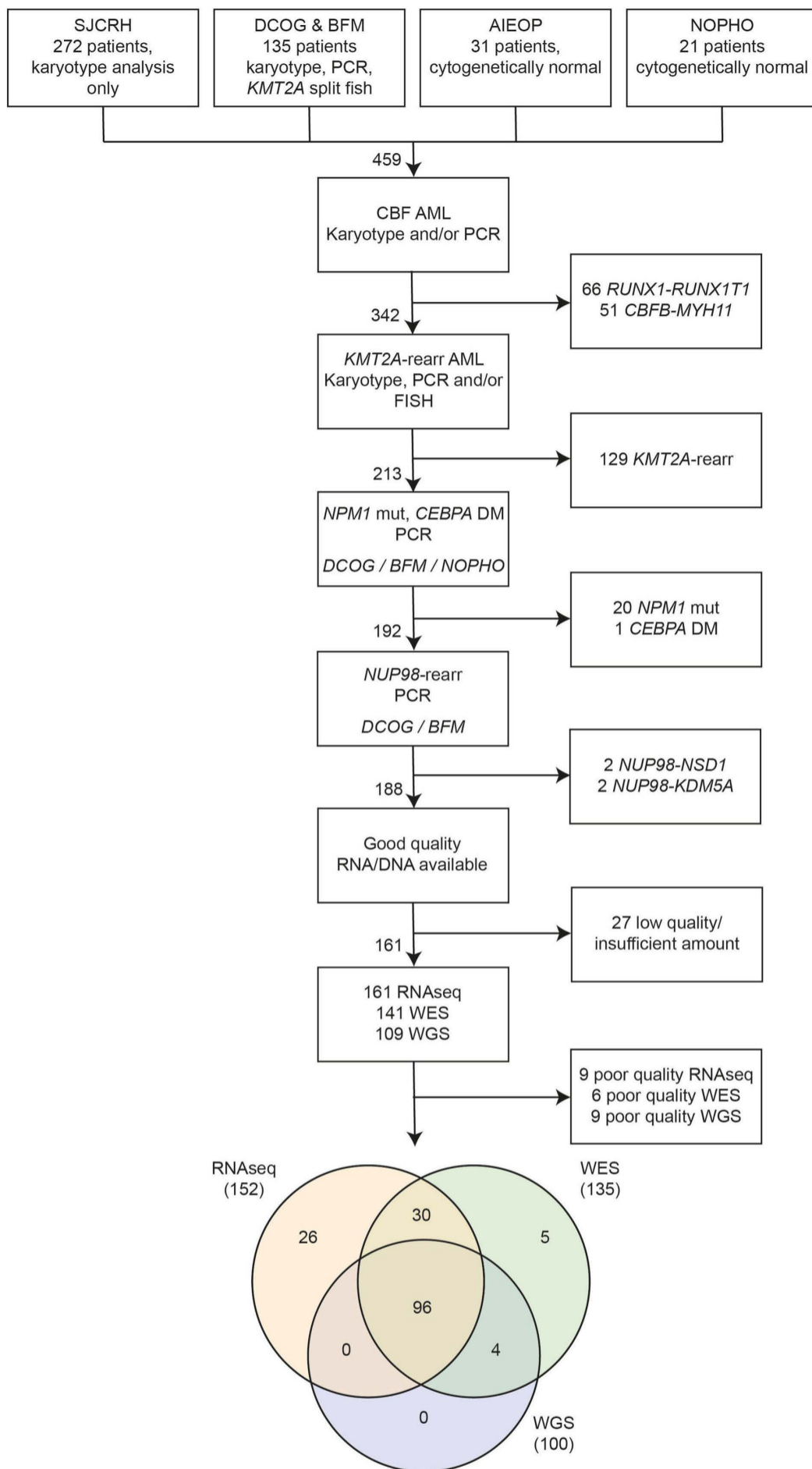


Figure 1. Flow diagram of the cohort selection. Patients from different cohorts were selected according to the research groups diagnostic procedures. Patient samples from SJCRH were selected based on karyotype analysis only, patient samples from DCOG and BFM were selected based on karyotype analysis and molecular analysis such as reverse transcription polymerase chain reaction (RT-PCR) and *KMT2A* split-fluorescence *in situ* hybridization analysis. NOPHO and AIEOP both provided samples from patients with a normal karyotype, of whom NOPHO excluded *NPM1* mutated patients. In total 161 patients had good quality RNA sequencing (RNAseq) (n=152), whole exome sequencing (WES) (n=135) and/or whole genome sequencing (WGS) (n=100). SJCRH: St Jude Children's Research Hospital; DCOG: Dutch Childhood Oncology Group; BFM: Berlin-Frankfurt-Münster Group; NOPHO: Nordic Society of Pediatric Hematology and Oncology; AIEOP: Associazione Italia di Ematologica e Oncologia Pediatrica. FISH: Fluorescence *in situ* hybridization; mut: mutated; rearr: rearrangement.

Results

Fusion detection

In total, 156 of 161 (97%) of analyzed patients had RNAseq and/or WGS data. Of these, fusion genes were identified in 71 patients (44%) (Table 1), confirming the high frequency of translocation events in pediatric AML. Due to the different selection processes of the cohorts, several well-known drivers were detected that were not detected by the re-

search groups using the conventional diagnostic cytogenetic screening methods, like *CBFB-MYH11* (n=2), *KMT2A* rearrangements (n=23), and cryptic *NUP98* rearrangements (n=12). Additionally, in 13 patients other rearrangements were identified: *DEK-NUP214* in three patients, *FUS-ERG* (n=4), *CREBBP-KAT6A* (n=2), *KMT2A-PTD* (n=2) and enhancer hijacking of *MECOM* (n=2), leaving ultimately 21 patients (13%) with novel fusions that are either unique or have only been scarcely reported in the literature. These

rearrangements involved *NPM1* (n=4), *ETV6* (n=4), *BCL11B* (n=2) and *GATA1* (n=2) (Table 1). One of the *BCL11B* rearrangements involved enhancer highjacking detected through WGS, showing a translocation between chromo-

Table 1. Characteristics of rearrangements detected in this cohort. This table depicts the characteristics of patients with rearrangements detected in this cohort.

| Rearrangements | Patients N | Median age in years (range) | FAB type | | | | | | |
|------------------------------------|------------|-----------------------------|----------|---------|---------|---------|---------|---------|---------|
| | | | M0 (%) | M1 (%) | M2 (%) | M4 (%) | M5 (%) | M6 (%) | NOS (%) |
| All patients | 161 | 11.0 (0.3-21.3)** | 9 (5.5) | 42 (26) | 30 (19) | 28 (17) | 32 (20) | 4 (2.5) | 18 (11) |
| KMT2A rearrangements | 23 | 3.4 (0.3-15.6) | | 2 (9) | | 5 (22) | 13 (56) | | 4 (13) |
| <i>KMT2A-MLLT10</i> | 9 | 3.5 (0.4-13.0) | | | | 1 | 8 | | |
| <i>KMT2A-MLLT4</i> | 3 | 8.7 (3.1-14.6) | | | | 1 | 1 | | 1 |
| <i>KMT2A-ELL</i> | 2 | 3.3 (0.4-6.2) | | 1 | | 1 | | | |
| <i>KMT2A-MLLT1</i> | 2 | 1.9 (0.3-3.4) | | | | | 2 | | |
| <i>KMT2A-PTD</i> | 2 | 13.4 (11.2-15.6) | | | | 1 | | | 1 |
| <i>KMT2A-SEPT6</i> | 2 | 3.5 (1.6-5.3) | | 1 | | | 1 | | |
| <i>KMT2A-USP2</i> | 1 | 1.3 | | | | | | | 2 |
| <i>KMT2A-EPS15</i> | 1 | 2.1 | | | | 1 | | | |
| <i>KMT2A-MLLT3</i> | 1 | 2.1 | | | | | 1 | | |
| NUP rearrangements | 14 | 12.0 (1.8-19.9) | | 1 (7) | 3 (21) | 3 (21) | 3 (21) | 1 (7) | 3 (21) |
| <i>NUP98-NSD1</i> | 8 | 12.9 (6.7-19.9) | | | 2 | 3 | 1 | | 2 |
| <i>DEK-NUP214</i> | 3 | 14.2 (11.5-14.3) | | | 1 | | 1 | | 1 |
| <i>NUP98-KDM5A</i> | 2 | 6.0 (1.8-10.1) | | | | | 1 | 1 | |
| <i>NUP98-HOXA13</i> | 1 | 2.3 | | 1 | | | | | |
| ERG rearrangements | 6 | 8.0 (2.6-12.8) | | 1 (17) | 1 (17) | | 3 (50) | | 1 (17) |
| <i>FUS-ERG</i> | 4 | 5.5 (2.6-9.2) | | | 1 | | 2 | | 1 |
| <i>FUS-FEV</i> | 1 | 12.8 | | 1 | | | | | |
| <i>EWSR1-ERG</i> | 1 | 8.7 | | | | | 1 | | |
| NPM1 rearrangements | 4 | 3.2 (0.7-3.4)* | | 1 (25) | 1 (25) | | 1 (25) | | 1 (25) |
| <i>NPM1-CCDC28A</i> | 3 | 2.0 (0.7-3.2)* | | | 1 | | 1 | | 1 |
| <i>NPM1-HAUS1</i> | 1 | 3.4 | | 1 | | | | | |
| ETV6 rearrangements | 4 | 7.2 (0.8-16.4) | 1 (25) | 2 (50) | 1 (25) | | | | |
| <i>ETV6-SMARCA2</i> | 1 | 1.6 | | | 1 | | | | |
| <i>ETV6-MECOM</i> | 1 | 16.4 | | 1 | | | | | |
| <i>ETV6-LRP6</i> | 1 | 12.7 | | 1 | | | | | |
| <i>MNX1-ETV6</i> | 1 | 0.8 | 1 | | | | | | |
| CREBBP-KAT6A | 2 | 10.4 (1.5-19.3) | | | | 2 (100) | | | |
| CBFB-MYH11 | 2 | 9.6 (3.0-16.3) | | | | 2 (100) | | | |
| MECOM | 2 | 6.0 (4.6-7.5) | 1 (50) | | | 1 (50) | | | |
| BCL11B rearrangements | 2 | 5.0 (3.8-6.2) | | | | | | | 2 (100) |
| <i>BCL11B-ZEB2</i> | 1 | 6.2 | | | | | | | 1 |
| <i>BCL11B enhancer highjacking</i> | 1 | 3.8 | | | | | | | 1 |
| GATA1 | 2 | 1.0 (0.6-1.3) | | | 2 (100) | | | | |
| <i>GATA1 deletion exon 2-4</i> | 1 | 1.3 | | | 1 | | | | |
| <i>MYB-GATA1</i> | 1 | 0.6 | | | 1 | | | | |
| CBFA2T3-GLIS2 | 1 | 1.2 | 1 (100) | | | | | | |
| EWSR1-ZNF384 | 1 | 13.8 | | | 1 (100) | | | | |
| FOSB-KLF6 | 1 | 16.6 | | 1 (100) | | | | | |
| MED12-HOXA9 | 1 | 17.7 | | 1 (100) | | | | | |
| PICALM-MLLT10 | 1 | 11.0 | | | | | | | 1 (100) |
| PIM1-BRD1 | 1 | 10.6 | | | 1 (100) | | | | |
| RUNX1-USP42 | 1 | 16.8 | | | | 1 (100) | | | |
| SFPQ-ZFP36L2 | 1 | 12.4 | | 1 (100) | | | | | |
| ZEB2-CTDSP1 | 1 | 11.5 | | | 1 (100) | | | | |
| PER2 | 1 | - | | | | | | | 1 (100) |

*data missing for 1 patient, ** data missing for 2 patients.

some 8 and 14. The break point of chromosome 8 was in an intronic region of *CCDC26*, which is the same location of the t(3;8) translocation involving MECOM enhancer hijacking.²² One of the genes closest to the genomic break point on chromosome 14 was *BCL11B* and displayed high gene expression, whereas other genes close to the genomic break point were not affected.

Mutations

WES data was available for 134 of 161 (83%) patients and both WES and WGS data was available for 101 patients. As germline material was used as a reference, only somatic mutations were considered. The median number of mutations with functional consequences in coding regions, i.e., changes in the amino acid composition of the protein, was 23.0 (range, 7-116) per patient. In total, 3,070 unique genes harbored mutations, of which 512 (17%) genes were mutated in at least two patients.

Most of these recurrent mutations had been previously described, such as *FLT3* (n=35, 27%), *NRAS* (n=25, 18%), *CEBPA* (n=22, 16%), *WT1* (n=20, 15%), *NPM1* (n=15, 10%), *KRAS* (n=9, 6%) and *RUNX1* (n=8, 6%) (Figure 2A; Table 2). Single gene mutations commonly found in adult AML were rare in this cohort, i.e., *IDH1* and *IDH2* mutations both occurred in 3.0% of patients (4/134), *ASXL1* in 2.2% (3/134), *DNMT3A* in 1.5% (2/134), *TET2* in 1.5% (2/134), and *EZH2* in 1.5% (2/134) of patients.

Novel recurrent mutations involved *TTN* (n=18, 13%), *UBTF* (n=10, 8%), *TCHH* (n=9, 7%) and *SRA1* (n=9, 7%). As *TTN* and *TCHH* are large genes and are often mutated in a variety of cancers without clinical consequences, these mutations were not further analyzed.

Mutations in the *UBTF* gene had not been previously described in pediatric AML, but rearrangements involving this gene have been described in prostate cancer.²³ All mutations detected in *UBTF* occurred in exon 13. In total, four patients had a tandem duplication, three patients had in frame deletions, of whom one also had a missense mutation, four patients had missense mutations and one patient had a mutation in the splice region. Patients with a mutation in *UBTF* had a median variant allele frequency (VAF) of 16.1 (range 10.2-35.6). In five of ten *UBTF*-mutated patients a mutation in *WT1* was detected, and one patient had a concomitant *CEBPA* DM.

Another novel mutated gene in nine pediatric AML cases was *SRA1*. Mutations occurred with a median VAF of 100 (range, 39-100), and all were missense mutations, and resulted in the same amino acid change (V110L). This mutation is registered in the COSMIC database and is predicted to be benign with SIFT and Polyphen scores of 0 (Online Supplementary Table S2).

Non-random association between aberrations

A non-random association between several type I and

type II aberrations was detected (Figure 2A). As previously described, *FLT3*-ITD was associated with *NPM1* mutations (9/35, 26%, $P=0.001$), and *WT1* (8/35, 23%, $P=0.047$) mutations.¹⁰ Furthermore, patients with mutations in *CEBPA* had a higher frequency of *GATA2* mutations compared to the remaining cohort (27%, $P<0.001$). Of the patients with both *CEBPA* and *GATA2* mutations, three concerned biallelic *CEBPA* mutations and three monoallelic mutations (Online Supplementary Figure S1). Another association was found between *NPM1* mutations and mutations in *RAD21* (3/15, 20%, $P<0.001$). A novel association was detected between *CEBPA* mutations and mutations in *KMT2C* (n=3, 14%, $P=0.002$).

Copy number alterations

Both WES and WGS data were used to identify copy number alterations, such as chromosome 7 or 7q deletions (n=5), chromosome 8 gain (n=5) and chromosome 5q loss (n=4) (Online Supplementary Figure S2). The most common copy number alteration in this cohort involved a gain of chromosome 1q (n=7). A focal deletion was detected in chromosome 16 involving the *CTCF* gene in three patients, and one patient had a heterozygous deletion of chromosome 16q. Furthermore, WGS analysis identified chromotrypsis in chromosome 8, 12 and 19 in three individual patients.

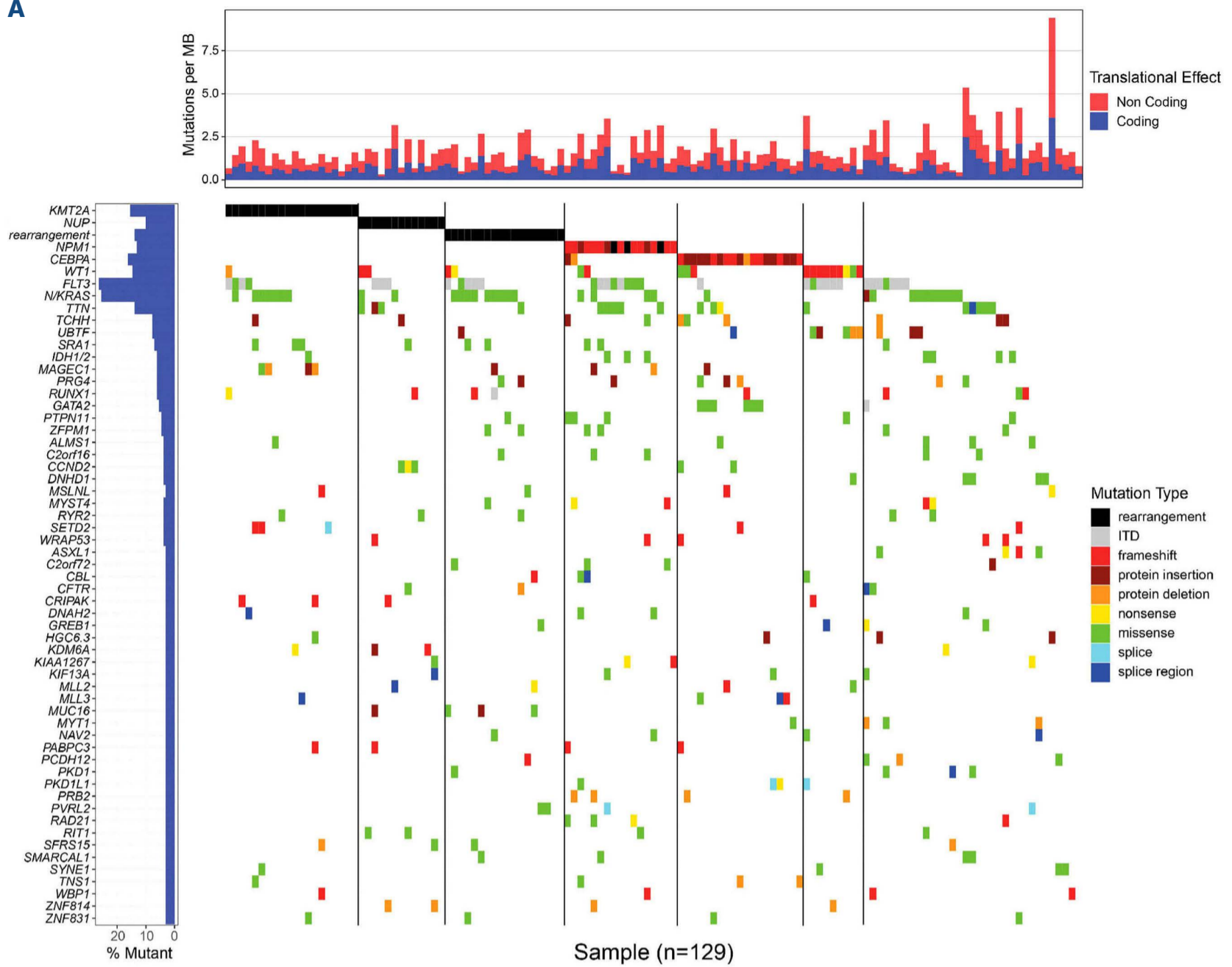
Gene expression analysis

Unsupervised clustering, using T-SNE on 152 patients with RNAseq data, revealed six clusters (Figure 2B). As was previously described, *KMT2A* rearrangements and *CREBBP-KAT6A* clustered together.²⁴

Furthermore, a large cluster containing 67 patients, was characterized by a high expression of *HOXA/B* genes. Aberrations such as *NPM1* mutations and rearrangements (n=19), *NUP98* rearrangements (n=10), *DEK-NUP214* (n=3) and *KMT2A* rearrangements (n=5), were detected in this cluster, as reported before.¹² Also mutations in *WT1* (13/19, 68%) and *FLT3*-ITD (23/35, 66%) were enriched in this cluster (Online Supplementary Figure S3). In total, six patients had both *WT1* and *FLT3* mutations, of which five had no other rearrangement or mutation in *NPM1* or *CEBPA*. Furthermore, this cluster appeared subdivided into two 'subclusters', which might be explained by the morphological subtype (FAB type), as one is enriched in granulocytic leukemias (FAB M1/M2) and the other in leukemias from myelo-monocytic origin (FAB M4/M5) (Online Supplementary Figure S4).

Although only double mutations of *CEBPA* have been described to have a distinct gene expression pattern, in this cohort, both single (n=12) and double mutations (n=8) clustered together based on gene expression.²⁵ In total, 18 of 20 *CEBPA* mutated cases with RNAseq data clustered together. The two patients that clustered separately

A



B

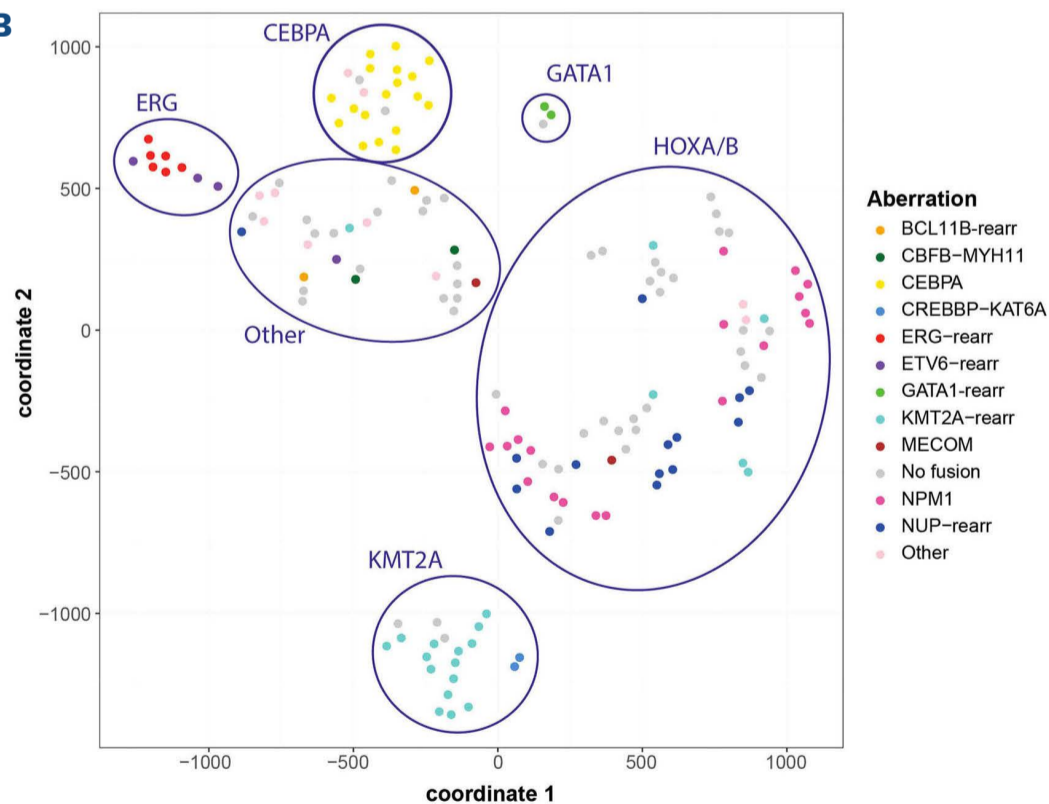


Figure 2. Integrative analysis of mutations and gene expression. (A) Waterfall plot of recurrent mutations occurring in at least 4 patients, mutations occurring in less than 3 patients were excluded from this analysis. The plot was first ordered based on type II aberration. Rearrangements occurring less than 5-times were taken together. From FLT3 downward, genes were ordered based on the number of mutations that occurred. (B) t-distributed stochastic neighbor embedding (T-SNE) analysis using the top 200 most variant genes based on standard deviation of 153 patients with RNA-sequencing data. ITD: internal tandem repeat; rearr: rearrangement.

Table 2. Characteristics of mutations detected in this cohort. This table depicts the characteristics of mutations that occur in at least 8 patients in this cohort.

| Mutations | Patients N | Median age in years (range) | FAB type | | | | | | |
|--------------|------------|-----------------------------|----------|---------|--------|---------|--------|--------|---------|
| | | | M0 (%) | M1 (%) | M2 (%) | M4 (%) | M5 (%) | M6 (%) | NOS (%) |
| <i>FLT3</i> | 35 | 12.8 (0.4-21.2)* | 1 (3) | 9 (26) | 4 (11) | 11 (31) | 6 (17) | | 5 (14) |
| <i>NRAS</i> | 25 | 11.7 (0.4-19.9) | | 4 (16) | 5 (20) | 8 (32) | 7 (28) | 1 (4) | |
| <i>CEBPA</i> | 21 | 12.7 (3.9-21.3) | | 13 (62) | 2 (9) | 1 (5) | 3 (14) | | 2 (10) |
| <i>WT1</i> | 20 | 12.3 (3.9-19.9) | 1 (5) | 7 (35) | 6 (26) | | 3 (15) | 1 (5) | 3 (15) |
| <i>TTN</i> | 19 | 12.4 (0.7-19.9) | 2 (11) | 6 (32) | 5 (26) | 2 (10) | 3 (16) | | 1 (5) |
| <i>NPM1</i> | 15 | 13.9 (4.4-21.2) | | 2 (13) | 4 (27) | 5 (34) | 2 (13) | | 2 (13) |
| <i>UBTF</i> | 10 | 12.2 (4.0-16.4) | | 1 (10) | 4 (40) | 3 (30) | | 2 (20) | |
| <i>SRA1</i> | 9 | 11.9 (1.3-19.3) | | 1 (11) | | 3 (33) | 3 (33) | | 2 (22) |
| <i>TCHH</i> | 9 | 13.3 (3.9-16.6) | | 3 (33) | 3 (33) | 1 (11) | 2 (22) | | |
| <i>KRAS</i> | 9 | 2.1 (0.7-16.8) | 1 (11) | | 1 (11) | 2 (22) | 5 (56) | | |
| <i>RUNX1</i> | 8 | 13.1 (3.8-19.0) | | 5 (63) | | 2 (25) | | | 1 (12) |

had a single mutation in *CEBPA* and an additional *NPM1* mutation.

Furthermore, a small cluster of nine samples could be detected, which was enriched with *ERG* rearrangements. Of these nine patients that clustered together, four had a *FUS-ERG* rearrangement, one a *FUS-FEV* rearrangement and one a *EWSR1-ERG* rearrangement. The three other patients had an *ETV6* rearrangement.

A small “cluster” consisted of only three samples of which two had a rearrangement involving *GATA1*.

The patients in the remaining cluster, carried various non-recurrent rearrangements, including *BCL11B* rearrangements (n=2), *CBFB-MYH11* (n=2), *ETV6-MECOM* (n=1), *KMT2A-MLLT10* (n=1), *MECOM* (n=1), *NUP98-HOXA13* (n=1), *SFPQ-ZFP36L2* (n=1), *MED12-HOXA9* (n=1), *PIM1-BRD1* (n=1), *CBFA2T3-GLIS2* (n=1), *PICALM-MLLT10* (n=1), *RUNX1-USP42* (n=1).

Clinical outcome

Survival data was available of 151 of 161 patients (94%). Surviving patients had a median follow-up time of 6.7 years (range, 0.1-14.5). The entire cohort had a 5-year EFS of 50% (standard error [SE]=4%) and OS of 67% (SE=4%). When patients were stratified according to genetic aberration, trends in differences in outcome were observed (Figure 3). Patients with *CEBPA* mutations and *NPM1* mutations or rearrangements had a 5-year EFS of 71% (SE=10%) and 82% (SE=5%), respectively, the 5-year OS rates were 89% (SE=7%) in both groups. In order to investigate survival of patients with *CEBPA* mutations, they were split up between single (n=9) and double mutations (n=9) (Online Supplementary Figure S5). Patients with *CEBPA* DM had no events or deaths, however, patients with *CEBPA* SM had an EFS of 56% (SE=16%) and OS of 80% (SE=12%). The difference in EFS between *CEBPA* SM and DM was significant ($P=0.03$). In contrast, patients with *ERG* rearrangements had a very poor outcome, i.e., all patients had an event within 2 years after diagnosis (1 refractory

disease, 4 relapses, 1 early death).

ERG rearrangements

ERG rearrangements were investigated in more detail as they were associated with a poor outcome. Patient characteristics were verified by combining the current data with the TARGET cohort.¹⁰ The TARGET cohort contained seven pediatric patients with a rearrangement involving *ERG* or another *ETS* transcription factor of the *ERG* subgroup, namely four *FUS-ERG*, two *FUS-FEV* and one *FUS-FLI1*. Combining data confirmed the dismal outcome of these patients as in total 11 of 13 patients had an event, and ten of 13 died (Figure 4A). The three surviving patients had a relatively short median follow-up time of 2.6 months (range, 2.0-31) (Online Supplementary Table S3). Furthermore, the date of diagnosis was not significantly different from patients who died ($P=0.17$). Multivariable analysis was unfeasible due to the limited number of patients. WES and/or WGS data was available in nine of 13 patients. Recurrent mutations occurred in N/*KRAS* (4/9) and *WT1* (2/9). No other genes were recurrently mutated. Differential gene expression analysis comparing *ERG*-rearranged AML to the remaining AML cohort revealed 1,034 significantly differentially expressed genes, of which 413 genes were upregulated and 621 genes were downregulated (Online Supplementary Table S4). Performing GSEA revealed upregulation of gene sets derived from (embryonic) stem cells and Ewing sarcoma (Figure 4A; Online Supplementary Table 5 and 6). As GSEA of the cluster enriched for *ERG* rearrangements revealed upregulation of genes involved in Ewing sarcoma, gene expression was compared between AML and a historic Ewing sarcoma RNAseq dataset using the top 50 differentially expressed genes of *ERG*-rearranged AML versus other AML.²⁶ Using hierarchical clustering, *ERG*-rearranged AML clustered closely to Ewing sarcoma samples and showed similar expression patterns, whereas other AML samples had opposing gene expression profiles (Figure 4B).

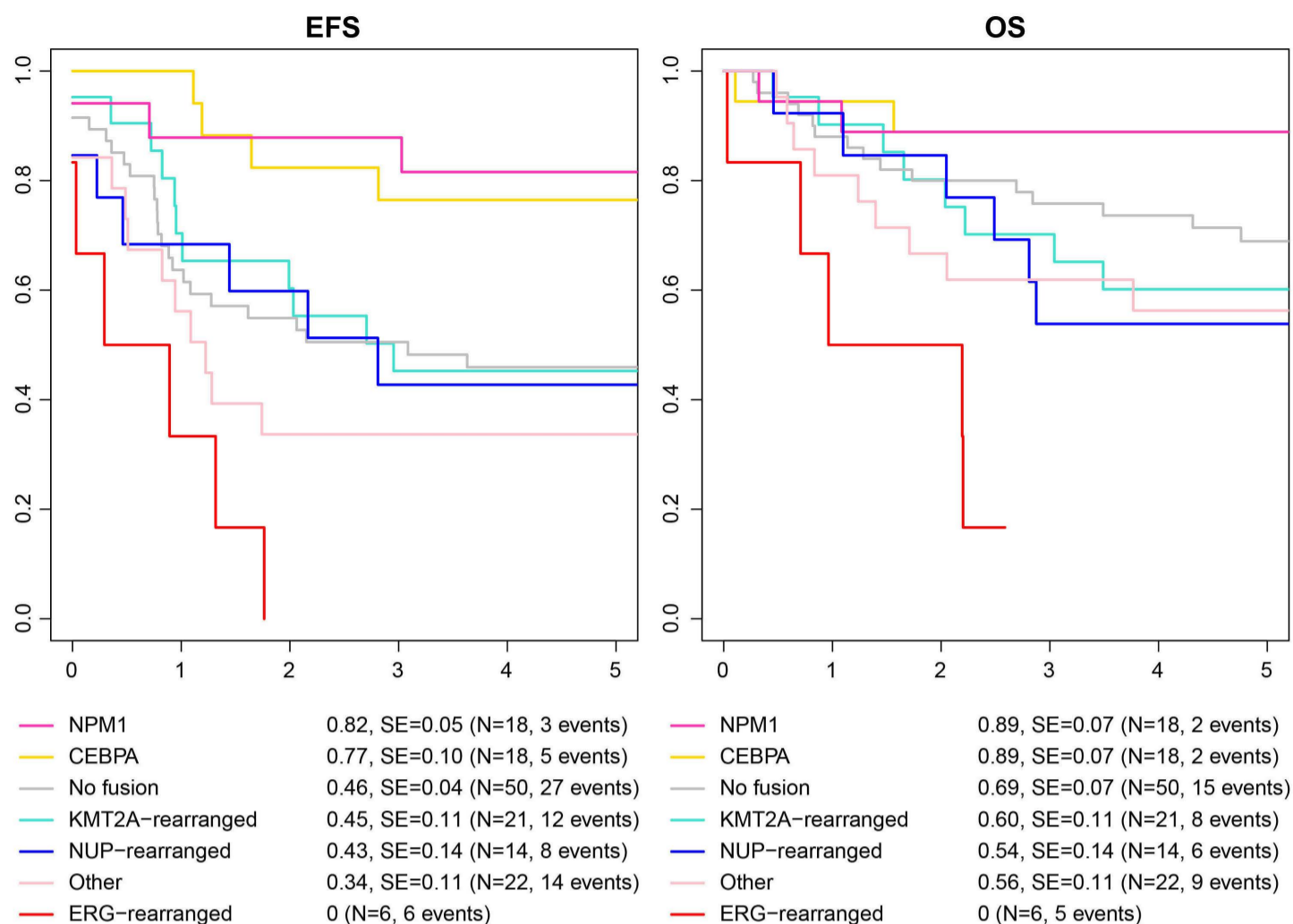


Figure 3. Patient outcome. (A) Event-free survival (EFS) and (B) overall survival (OS) of patients stratified by driving aberration. Aberrations that occur less than 5-times in this cohort have been combined with other rearrangements.

In order to investigate the transforming capacity of *ERG* rearrangements, *FUS-ERG*, *FUS-FEV* and *EWSR1-ERG* fusions were transduced into murine lineage depleted bone marrow cells and cultured using the colony-forming assay. *FUS-ERG* and *EWSR1-ERG* showed self-renewal capacity beyond the cells transduced with an empty vector. However, we could not demonstrate this for *FUS-FEV* (Figure 4B), suggesting a second hit might be needed for this rearrangement.

***NPM1* rearrangements**

In total 21 patients had an event in *NPM1*, of whom 17 had a mutation and four had an *NPM1*-rearrangement (3 *NPM1-CCDC28A* and 1 *NPM1-HAUS1*). Of the *NPM1*-rearranged cases, follow-up data was available for three patients, who were all alive at the last follow-up with a median follow-up time of 3.5 years (range, 3.1-7.2).

Differential gene expression analysis comparing *NPM1* mutated and rearranged cases to the remaining cohort revealed 1,437 significantly differentially expressed genes, of which 251 genes were upregulated and 1,186 genes were downregulated (*Online Supplementary Table S7*). When *NPM1*-mutated and *NPM1*-rearranged cases were separately compared to *NPM1*-wild-type patients, this revealed 421 and 113 differentially expressed genes, respectively (*Online Supplementary Tables S8* and *S9*). GSEA revealed

upregulation of gene sets derived from *NPM1* mutated AML for both *NPM1*-mutated and *NPM1*-rearranged gene sets (Figure 5A to C; *Online Supplementary Tables S10* and *S11*). *NPM1* mutations cause *NPM1* retainment in the cytoplasm.²⁷ In order to investigate whether *NPM1* rearrangements also resulted in cytoplasmic *NPM1*, immunofluorescent staining of *NPM1* was performed on cytopins of primary AML patients with or without *NPM1* mutations and rearrangements and compared to a sample of peripheral blood from a healthy donor. Cytoplasmic staining could be detected in AML samples with either *NPM1* mutations or *NPM1* rearrangements (Figure 5D), in contrast to *NPM1*-wild-type AML samples and healthy peripheral blood, where the staining was mainly localized in the nucleoli.

Discussion

This collaborative study aimed to identify novel genetic aberrations in pediatric AML without known type 2 aberrations using routine clinical diagnostics, which varied among the participating collaborative groups in this study as they all used a slightly different approach to standard diagnostics. In approximately 45% of cases a rearrangement could be detected, emphasizing the fusion driven

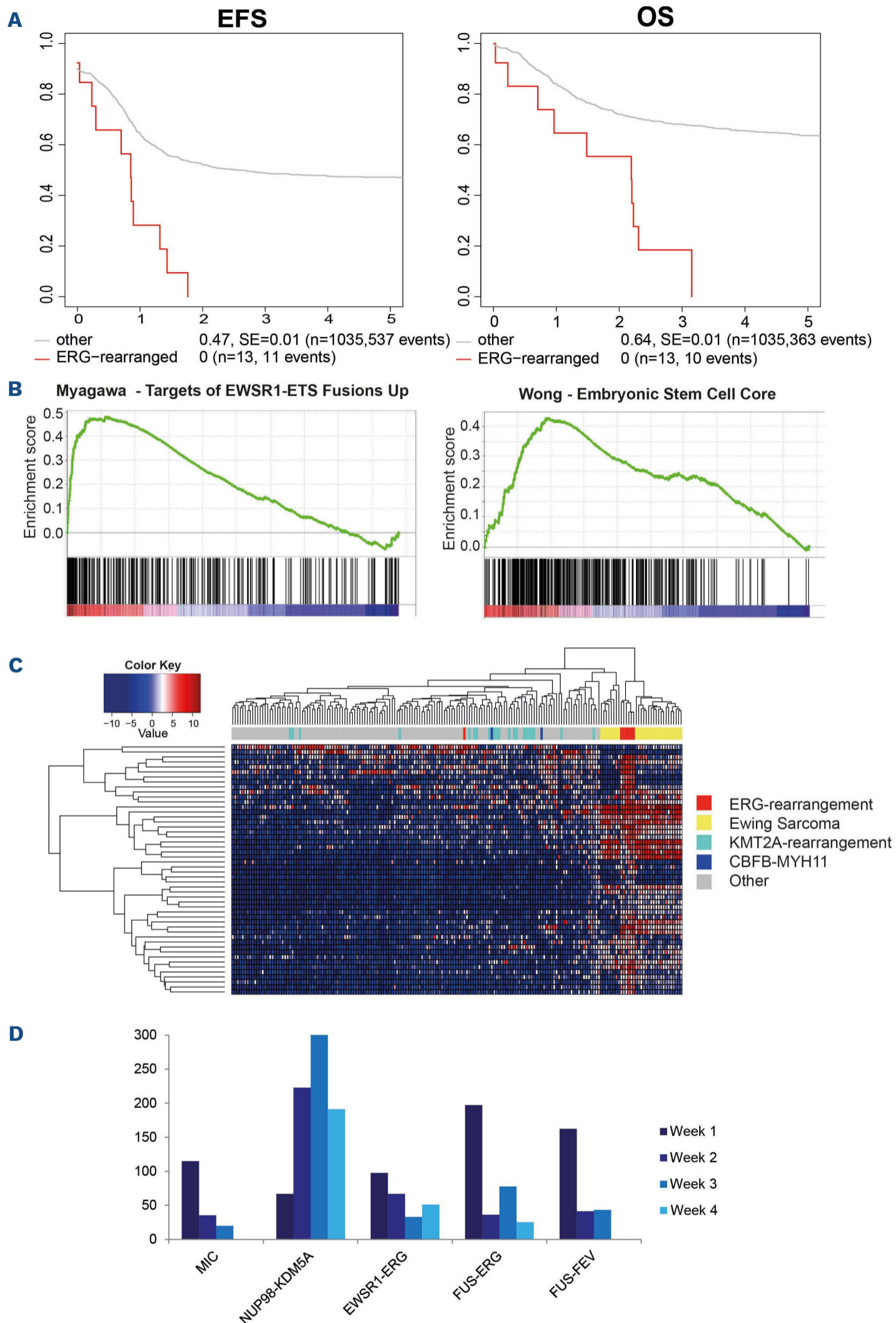


Figure 4. Characteristics of *ERG*-rearranged acute myeloid leukemia. (A) Survival curves combining data from Bolouri *et al.* and this cohort, comparing survival of *ERG*-rearranged acute myeloid leukemia (AML) to the remaining cohort. (B) Gene set enrichment analysis plots of gene sets derived from *EWSR1-FLI1* targets and embryonic stem cells. (C) Hierarchical clustering of AML and Ewing sarcoma samples using the top 50 differentially expressed genes of *ERG*-rearranged AML vs. other AML (absolute log-fold change). Ewing sarcoma samples cluster together with *ERG*-rearranged AML. (D) Colony-forming assay of *ERG* and *FEV* rearrangements detected in AML. *NUP98-KDM5A* was taken along as a positive control. Expression of *EWSR1-ERG* and *FUS-ERG* in murine lin- cells resulted in repetitive replating. EFS: event-free survival; OS: overall survival.

nature of pediatric AML, versus the relatively high frequency of single-gene mutations in adult AML.²⁸ Some were well-known recurrent events, such as *KMT2A* rearrangements, others were previously described and known as rare events in pediatric AML, such as *DEK-NUP214* and *FUS-ERG*.^{29,30} Moreover, several novel or scarcely reported recurrent and some unique rearrangements were detected, such as rearrangements involving *BCL11B*, *GATA1* and *ETV6*. Of the patients without a known type II event, 30% (25/84) had a novel or unique rearrangement.

Besides rearrangements, WES and WGS detected a median of 24 coding mutations per patient, which is comparable to the mutational burden reported by Bolouri et al.¹⁰ In detail, we detected 502 recurrently mutated genes. Most of the recurrently mutated genes are well known, such as *N/KRAS*, *WT1*, *CEBPA*, *NPM1* and *FLT3*. Novel recurrent mutations were detected in the *UBTF* (n=10) and *SRA1* genes (n=9). *SRA1* or Steroid Receptor RNA Activator 1 encodes both a protein and long non-coding RNA (lncRNA). The lncRNA acts as an RNA coactivator, and is associated with breast cancer, whereas the encoded protein SRAP is

involved in splicing and cell cycle regulation.³¹⁻³³ As mutations in *SRA1* were predicted to be benign, we do not expect these mutations to be important pathogens. The *UBTF* gene on the other hand, encodes a protein which regulates mRNA transcription by RNA polymerase 1 or 2 and is associated with developmental neuro-regression.^{34,35} *UBTF* has been described as a translocation partner of *ETV1* or *ETV4* in prostate cancer. Furthermore, depletion of *UBTF* is associated with DNA damage and genomic instability.³⁶ However, there was no significant difference in the number of mutations between *UBTF*-mutated and wild-type cases. Patients with a mutation in *UBTF* clustered in the cluster with high *HOXA/B* expression (n=9), except for a patient with a *CEBPA* DM and *UBTF* mutation. Five of these patients had an additional *WT1* mutation, and one patient had an enhancer hijacking of *MECOM*. It is unlikely that this mutation is a type II aberration as it occurs subclonally with variant allele frequencies between 10.2% and 35%. Both mutations have not been described by Bolouri et al. and their transforming capacity is unknown.¹⁰ Due to the selection criteria of our cohort, patients with more rare aberrations and mu-

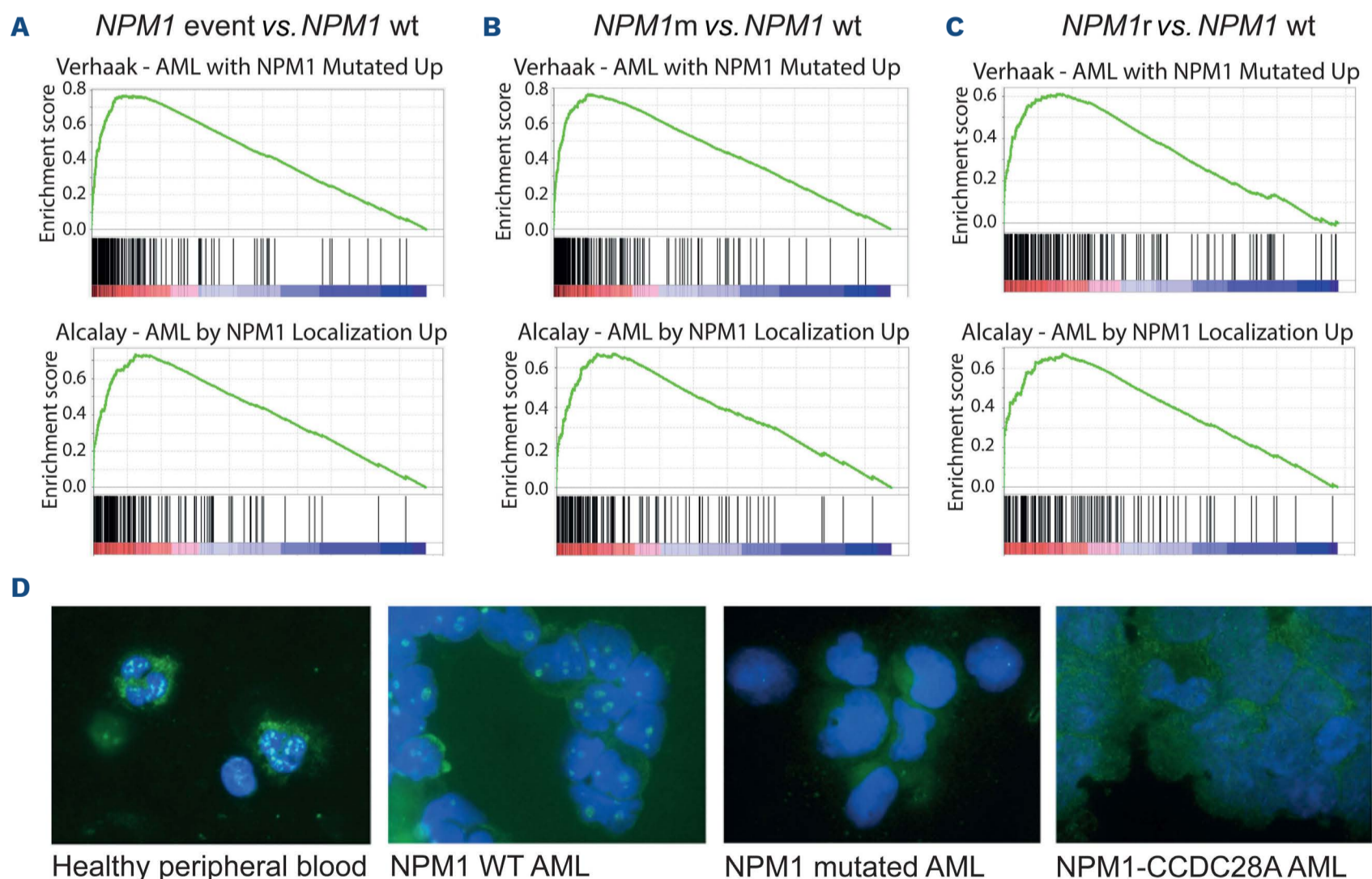


Figure 5. Characteristics of *NPM1*-rearranged acute myeloid leukemia. (A to C) Gene set enrichment analysis plots of gene sets upregulated in samples with an event in *NPM1* compared to samples without an event in *NPM1* (*NPM1* wild-type [wt]), of which (A) depicts all *NPM1* events (both rearrangements and mutations) vs. *NPM1* wt, (B) depicts *NPM1* mutations vs. *NPM1* wt, and (C) depicts *NPM1* rearrangements (*NPM1*r) vs. *NPM1* wt. (D). Cytospins of primary patient material stained with anti-*NPM1*. *NPM1* is located in the nucleoli in healthy peripheral blood and in an acute myeloid leukemia (AML) sample with *NPM1* wt, whereas it is localized in the cytoplasm in the *NPM1*-mutated and *NPM1*-rearranged AML samples.

tations are enriched in this cohort, which may attribute to the detection of recurrent mutations that were not previously described by studies using the same technique. In contrast to previous studies, a similar gene expression pattern of *CEBPA* DM and SM was detected.²⁵ However, in previous studies, *CEBPA* SM was associated with other type II aberrations such as *NPM1* mutations, which could result in differences in gene expression^{14,25} Furthermore, we did find a significant difference in EFS with a worse outcome in the *CEBPA* SM group, which was in contrast to a study by Tarlock *et al.*, who found no difference in outcome between *CEBPA* SM and DM.³⁷ However, our study was small with only nine patients in each group, whereas Tarlock *et al.* has a much larger study, and is potentially more reliable.

One patient subset was characterized by poor outcome, i.e., those with rearrangements in *FUS-ERG* (n=4), *EWSR1-ERG* (n=1) and *FUS-FEV* (n=1). *FUS-ERG*-rearranged AML has been described as a group with a poor outcome before,²⁹ which was reflected in this cohort and confirmed in the TARGET cohort by Bolouri *et al.* (Figure 4A).¹⁰ These rearrangements have also been described in Ewing sarcoma.^{10,26,29,38} The fusion genes involved the transcription factor binding site of *FUS* or *EWSR1*, and the DNA binding site of *ERG* or *FEV*. The fact that *FUS* and *EWSR1* are homologs and *ERG* and *FEV*, together with *FLI1*, belong to the same ETS subfamily, could explain why these rearrangements result in a similar gene expression pattern and cluster together in unsupervised clustering analysis (Figure 2B).^{39,40} GSEA revealed upregulation of pathways involved in stem cell development. This was expected as genes involved in these fusions are important for the regulation, development and self-renewal of hematopoietic stem cells.⁴¹⁻⁴⁶

In addition, expression signatures previously described in Ewing sarcoma were upregulated, and all fusions in this group also occur in Ewing sarcoma. When combining RN seq data from AML and Ewing sarcoma patients, the *ERG*-rearranged AML patients clustered together with Ewing sarcoma patients, whereas other AML patients clustered separately. This suggests that *ERG*-rearranged AML shares oncogenic pathways with Ewing sarcoma in contrast to other AML samples. Finding common ground between cancers can be useful for detecting novel therapeutic targets. Current chemotherapy protocols of AML and Ewing sarcoma are rather comparable, and not many additional novel therapeutic agents have proven to be effective.^{2,47,48} Another recurrent set of rearrangements included *NPM1* rearrangements (n=4). We detected two different types of rearrangements: *NPM1-CCDC28A* (n=3) and *NPM1-HAUS1* (n=1). Bolouri *et al.* also detected four patients with *NPM1* fusions, i.e., *NPM1-MLF1*.¹⁰ All three *NPM1*-rearranged patients with survival data in our cohort were in CCR, whereas of the four *NPM1*-rearranged patients in the TAR-

GET cohort, all patients relapsed and three patients subsequently died. Therefore, the prognostic value of *NPM1* rearrangements may be treatment or translocation partner dependent. The breakpoint of *NPM1* in the rearrangements in our study was between exon 11 and exon 12. As mutations and rearrangements both result in disruption of exon 12 of *NPM1*, we hypothesized that both events could result in cytoplasmic retention of *NPM1*, driving leukemogenesis in these cases.²⁷ Immunofluorescence of *NPM1* showed that *NPM1-CCDC28A* result in cytoplasmic retention of *NPM1* (Figure 5B). This has been previously shown for *NPM1-HAUS1* as well, which makes it likely that *NPM1* rearrangements and *NPM1* mutants functionally have a similar mechanism of action.⁴⁹ Furthermore, performing unsupervised clustering, all patients with an *NPM1* event clustered in the large cluster which is characterized by upregulation of *HOXA* and *HOXB*, further underlining the conceivable similarities in oncogenesis of *NPM1* mutations and rearrangements.

Rarer recurrent rearrangements involved *BCL11B* (n=2). *BCL11B* mutations and rearrangements are associated with T-ALL.^{50,51} In this cohort, one patient had a *ZEB2-BCL11B* rearrangement and in the other patient, enhancer hijacking of *BCL11B* was detected. Both rearrangements led to high expression of *BCL11B*. This rearrangement has been described in adult AML before, but did not lead to self-renewal capacity in CFU-GEM assay.⁵²

One of the drawbacks of this study is that 37% of the cases that were included in the study had a known driving genetic aberration, such as a *KMT2A* rearrangement, which was dependent on what was considered the diagnostic standard of care in the participating collaborative groups. This shows the relevance of implementing more genome-wide diagnostics, as for example karyotyping may appear not sufficient to detect all relevant fusions. Therefore, we suggest to implement NGS, i.e., RNAseq and WES, as standard of care in pediatric AML to readily detect driving aberrations, and stratify patients according to genetic events to improve outcome.⁵ Moreover, with the availability of targeted agents such as menin inhibitors, it becomes relevant to readily identify all *KMT2A* and *NUP98* rearrangements.

In 24% (n=39) of the patients in this study, despite NGS efforts, still no (potential) type II aberration could be identified. However, in eight of these 39 cases, only RN seq was performed, therefore, potentially driving single gene mutations could have been missed. As the mutational burden in coding regions of the genome in pediatric AML is low, we anticipate that potentially non-coding mutations may play an important role here, as well as epigenetic events.^{10,53}

In conclusion, this study has characterized several novel and rare genetic aberrations occurring in pediatric AML. Some novel rearrangements, such as *ERG* rearrangements

should be considered high risk, whereas for others, such as *NPM1* rearrangements this is not yet clear. Ideally for pediatric AML, diagnostics includes RNAseq when resources allow it, as we demonstrated that this detects rare relevant fusion genes with prognostic implications.

Disclosures

No conflicts of interest to disclose.

Contributions

CMZ, TAG, MF and MMvdH-E designed the study. DR, MP, FL, HH, JA, MJ, CK, SP, CMZ contributed materials and clinical

data. SN, MF, JM, MW and GS analyzed the data. SN, JvO and EARG performed experiments. SN and MF performed statistical analysis. SN, MF, MMvdH-E and CMZ wrote the paper. CMZ, MF, MMvdH-E and TAG supervised the study and all co-authors performed critical review of the manuscript and gave their final approval.

Data-sharing statement

Data for the sequenced samples in this study have been deposited to the St. Jude Cloud (www.stjude.cloud; ref. 33) and European Genome-phenome Archive (study ID EGAS00001004701).

References

- Rasche M, Zimmermann M, Borschel L, et al. Successes and challenges in the treatment of pediatric acute myeloid leukemia: a retrospective analysis of the AML-BFM trials from 1987 to 2012. *Leukemia*. 2018;32(10):2167-2177.
- Zwaan CM, Kolb EA, Reinhardt D, et al. Collaborative efforts driving progress in pediatric acute myeloid leukemia. *J Clin Oncol*. 2015;33(27):2949-2962.
- Rubnitz JE, Gibson B, Smith FO. Acute myeloid leukemia. *Hematol Oncol Clin North Am*. 2010;24(1):35-63.
- Rubnitz JE. Current management of childhood acute myeloid leukemia. *Paediatr Drugs*. 2017;19(1):1-10.
- Creutzig U, van den Heuvel-Eibrink MM, Gibson B, et al. Diagnosis and management of acute myeloid leukemia in children and adolescents: recommendations from an international expert panel. *Blood*. 2012;120(16):3187-3205.
- Gilliland DG, Jordan CT, Felix CA. The molecular basis of leukemia. *Hematology Am Soc Hematol Educ Program*. 2004:80-97.
- Balgobind BV, Hollink IH, Arentsen-Peters ST, et al. Integrative analysis of type-I and type-II aberrations underscores the genetic heterogeneity of pediatric acute myeloid leukemia. *Haematologica*. 2011;96(10):1478-1487.
- Kelly LM, Gilliland DG. Genetics of myeloid leukemias. *Annu Rev Genomics Hum Genet*. 2002;3:179-198.
- Welch JS, Ley TJ, Link DC, et al. The origin and evolution of mutations in acute myeloid leukemia. *Cell*. 2012;150(2):264-278.
- Bolouri H, Farrar JE, Triche T, Jr., et al. The molecular landscape of pediatric acute myeloid leukemia reveals recurrent structural alterations and age-specific mutational interactions. *Nat Med*. 2018;24(1):103-112.
- de Rooij JD, Branstetter C, Ma J, et al. Pediatric non-Down syndrome acute megakaryoblastic leukemia is characterized by distinct genomic subsets with varying outcomes. *Nat Genet*. 2017;49(3):451-456.
- Hollink IH, van den Heuvel-Eibrink MM, Arentsen-Peters ST, et al. NUP98/NSD1 characterizes a novel poor prognostic group in acute myeloid leukemia with a distinct HOX gene expression pattern. *Blood*. 2011;118(13):3645-3656.
- Tyner JW, Tognon CE, Bottomly D, et al. Functional genomic landscape of acute myeloid leukaemia. *Nature*. 2018;562(7728):526-531.
- Hollink IH, van den Heuvel-Eibrink MM, Arentsen-Peters ST, et al. Characterization of CEBPA mutations and promoter hypermethylation in pediatric acute myeloid leukemia. *Haematologica*. 2011;96(3):384-392.
- Hollink IH, Zwaan CM, Zimmermann M, et al. Favorable prognostic impact of *NPM1* gene mutations in childhood acute myeloid leukemia, with emphasis on cytogenetically normal AML. *Leukemia*. 2009;23(2):262-270.
- Ho PA, Kutny MA, Alonzo TA, et al. Leukemic mutations in the methylation-associated genes DNMT3A and IDH2 are rare events in pediatric AML: a report from the Children's Oncology Group. *Pediatr Blood Cancer*. 2011;57(2):204-209.
- Fornerod M, Ma J, Noort S, et al. Integrative genomic analysis of pediatric myeloid-related acute leukemias identifies novel subtypes and prognostic indicators. *Blood Cancer Discov*. 2021;2(6):586-599.
- Law CW, Chen Y, Shi W, Smyth GK. Voom: precision weights unlock linear model analysis tools for RNA-seq read counts. *Genome Biol*. 2014;15(2):R29.
- Subramanian A, Kuehn H, Gould J, Tamayo P, Mesirov JP. GSEA-P: a desktop application for gene set enrichment analysis. *Bioinformatics*. 2007;23(23):3251-3253.
- Subramanian A, Tamayo P, Mootha VK, et al. Gene set enrichment analysis: a knowledge-based approach for interpreting genome-wide expression profiles. *Proc Natl Acad Sci U S A*. 2005;102(43):15545-15550.
- Therneau TM. A package for survival analysis in R. 2020. Available from: <https://CRAN.R-project.org/package=survival>.
- Ottema S, Mulet-Lazaro R, Erpelinck-Verschueren C, et al. The leukemic oncogene *EVI1* hijacks a MYC super-enhancer by CTCF-facilitated loops. *Nat Commun*. 2021;12(1):5679.
- Barros-Silva JD, Paulo P, Bakken AC, et al. Novel 5' fusion partners of *ETV1* and *ETV4* in prostate cancer. *Neoplasia*. 2013;15(7):720-726.
- Coenen EA, Zwaan CM, Reinhardt D, et al. Pediatric acute myeloid leukemia with t(8;16)(p11;p13), a distinct clinical and biological entity: a collaborative study by the International-Berlin-Frankfurt-Munster AML-study group. *Blood*. 2013;122(15):2704-2713.
- Wouters BJ, Lowenberg B, Erpelinck-Verschueren CA, van Putten WL, Valk PJ, Delwel R. Double CEBPA mutations, but not single CEBPA mutations, define a subgroup of acute myeloid leukemia with a distinctive gene expression profile that is uniquely associated with a favorable outcome. *Blood*. 2009;113(13):3088-3091.
- Crompton BD, Stewart C, Taylor-Weiner A, et al. The genomic landscape of pediatric Ewing sarcoma. *Cancer Discov*. 2014;4(11):1326-1341.
- Heath EM, Chan SM, Minden MD, Murphy T, Shlush LI, Schimmer

- AD. Biological and clinical consequences of NPM1 mutations in AML. *Leukemia*. 2017;31(4):798-807.
28. DiNardo CD, Cortes JE. Mutations in AML: prognostic and therapeutic implications. *Hematology Am Soc Hematol Educ Program*. 2016;2016(1):348-355.
29. Noort S, Zimmermann M, Reinhardt D, et al. Prognostic impact of t(16;21)(p11;q22) and t(16;21)(q24;q22) in pediatric AML: a retrospective study by the I-BFM Study Group. *Blood*. 2018;132(15):1584-1592.
30. Sandahl JD, Coenen EA, Forestier E, et al. t(6;9)(p22;q34)/DEK-NUP214-rearranged pediatric myeloid leukemia: an international study of 62 patients. *Haematologica*. 2014;99(5):865-872.
31. Klinge CM. Non-coding RNAs in breast cancer: intracellular and intercellular communication. *Noncoding RNA*. 2018;4(4):40.
32. Leygue E. Steroid receptor RNA activator (SRA1): unusual bifaceted gene products with suspected relevance to breast cancer. *Nucl Recept Signal*. 2007;5:e006.
33. Sheng L, Ye L, Zhang D, Cawthorn WP, Xu B. New insights into the long non-coding RNA SRA: physiological functions and mechanisms of action. *Front Med (Lausanne)*. 2018;5:244.
34. Edvardson S, Nicolae CM, Agrawal PB, et al. Heterozygous de novo UBTF gain-of-function variant is associated with neurodegeneration in childhood. *Am J Hum Genet*. 2017;101(2):267-273.
35. Toro C, Hori RT, Malicdan MCV, et al. A recurrent de novo missense mutation in UBTF causes developmental neuroregression. *Hum Mol Genet*. 2018;27(4):691-705.
36. Sanij E, Diesch J, Lesmana A, et al. A novel role for the Pol I transcription factor UBTF in maintaining genome stability through the regulation of highly transcribed Pol II genes. *Genome Res*. 2015;25(2):201-212.
37. Tarlock K, Lamble AJ, Wang YC, et al. CEBPA-bZip mutations are associated with favorable prognosis in de novo AML: a report from the Children's Oncology Group. *Blood*. 2021;138(13):1137-1147.
38. Shing DC, McMullan DJ, Roberts P, et al. FUS/ERG gene fusions in Ewing's tumors. *Cancer Res*. 2003;63(15):4568-4576.
39. Andersson MK, Stahlberg A, Arvidsson Y, et al. The multifunctional FUS, EWS and TAF15 proto-oncoproteins show cell type-specific expression patterns and involvement in cell spreading and stress response. *BMC Cell Biol*. 2008;9:37.
40. Oikawa T, Yamada T. Molecular biology of the Ets family of transcription factors. *Gene*. 2003;303:11-34.
41. Cho J, Shen H, Yu H, et al. Ewing sarcoma gene Ews regulates hematopoietic stem cell senescence. *Blood*. 2011;117(4):1156-1166.
42. Lee J, Nguyen PT, Shim HS, et al. EWSR1, a multifunctional protein, regulates cellular function and aging via genetic and epigenetic pathways. *Biochim Biophys Acta Mol Basis Dis*. 2019;1865(7):1938-1945.
43. Liu TH, Tang YJ, Huang Y, et al. Expression of the fetal hematopoiesis regulator FEV indicates leukemias of prenatal origin. *Leukemia*. 2017;31(5):1079-1086.
44. Ng AP, Loughran SJ, Metcalf D, et al. Erg is required for self-renewal of hematopoietic stem cells during stress hematopoiesis in mice. *Blood*. 2011;118(9):2454-2461.
45. Sugawara T, Oguro H, Negishi M, et al. FET family proto-oncogene Fus contributes to self-renewal of hematopoietic stem cells. *Exp Hematol*. 2010;38(8):696-706.
46. Taoudi S, Bee T, Hilton A, et al. ERG dependence distinguishes developmental control of hematopoietic stem cell maintenance from hematopoietic specification. *Genes Dev*. 2011;25(3):251-262.
47. Grünwald TGP, Cidre-Aranaz F, Surdez D, et al. Ewing sarcoma. *Nat Rev Dis Primers*. 2018;4(1):5.
48. Whelan J, Le Deley MC, Dirksen U, et al. High-dose chemotherapy and blood autologous stem-cell rescue compared with standard chemotherapy in localized high-risk Ewing sarcoma: results of Euro-E.W.I.N.G.99 and Ewing-2008. *J Clin Oncol*. 2018;36(31):Jco2018782516.
49. Campregher PV, de Oliveira Pereira W, Lisboa B, et al. A novel mechanism of NPM1 cytoplasmic localization in acute myeloid leukemia: the recurrent gene fusion NPM1-HAUS1. *Haematologica*. 2016;101(7):e287-e290.
50. Kraszewska MD, Dawidowska M, Kosmalka M, et al. BCL11B, FLT3, NOTCH1 and FBXW7 mutation status in T-cell acute lymphoblastic leukemia patients. *Blood Cells Mol Dis*. 2013;50(1):33-38.
51. Przybylski GK, Dik WA, Wanzeck J, et al. Disruption of the BCL11B gene through inv(14)(q11.2q32.31) results in the expression of BCL11B-TRDC fusion transcripts and is associated with the absence of wild-type BCL11B transcripts in T-ALL. *Leukemia*. 2005;19(2):201-208.
52. Padella A, Simonetti G, Paciello G, et al. Novel and rare fusion transcripts involving transcription factors and tumor suppressor genes in acute myeloid leukemia. *Cancers (Basel)*. 2019;11(12):1951.
53. Conway O'Brien E, Prideaux S, Chevassut T. The epigenetic landscape of acute myeloid leukemia. *Adv Hematol*. 2014;2014:103175.